

Short communication

Fabrication of bilayered YSZ/SDC electrolyte film by electrophoretic deposition for reduced-temperature operating anode-supported SOFC

Motohide Matsuda^{a,*}, Takushi Hosomi^a, Kenji Murata^b, Takehisa Fukui^b, Michihiro Miyake^a

^a Graduate School of Environmental Science, Okayama University, 3-1-1 Tsushima-Naka, Okayama 700-8530, Japan

^b Hosowaka Powder Technology Research Institute, 1-9 Shoudai, Tajika, Hirakata, Osaka 573-1132, Japan

Received 22 September 2006; received in revised form 14 November 2006; accepted 22 November 2006

Available online 16 January 2007

Abstract

Bilayered Y₂O₃-stabilized ZrO₂ (YSZ)/Sm₂O₃-doped CeO₂ (SDC) electrolyte films were successfully fabricated on porous NiO–YSZ composite substrates by electrophoretic deposition (EPD) based on electrophoretic filtration followed by co-firing with the substrates. In EPD, positively charged YSZ and SDC powders were deposited directly on the substrates, layer by layer from ethanol-based suspensions. Delamination between YSZ and SDC films was avoided by reducing the SDC films' thickness to ca. 1 μm. A single cell was constructed on the bilayered electrolyte films composed of ca. 4 μm-thick YSZ and ca. 1 μm-thick SDC films. As a cathode in the cell, La_{0.6}Sr_{0.4}Co_{0.2}Fe_{0.8}O_{3-x} (LSCF) was used. Maximum output power densities greater than 0.6 W cm⁻² were obtained at 700 °C for the bilayered YSZ/SDC electrolyte cells thus constructed. © 2006 Elsevier B.V. All rights reserved.

Keywords: Solid oxide fuel cell; Electrophoretic deposition; Electrolyte film; Ceramic processing

1. Introduction

A recent trend in development of solid oxide fuel cells (SOFCs), which are efficient power generation devices with low pollutant emissions, is to lower the operating temperature to 650–800 °C with the objective of using alloys as interconnects. The operating temperature can be reduced either by reducing the thickness of the well-known YSZ electrolyte or by employing an alternative electrolyte such as (La, Sr)(Ga, Mg)O₃ and doped CeO₂ with oxide ion conductivities that are higher than that of YSZ. However, the (La, Sr)(Ga, Mg)O₃ presents the problem of material costs, and the doped CeO₂ electrolytes exhibit electron conduction, which degrades the cell performance in the operating temperature range. In contrast, the YSZ electrolyte is highly stable under usual operating conditions, and is more convenient to use than other electrolytes. Therefore, the application of YSZ electrolyte films is beneficial for development of reduced-temperature operating SOFCs.

The YSZ is, however, allowed to react easily with LSCF perovskite compound, which has often been used as a cath-

ode for reduced-temperature operating SOFCs. One approach to avoid the interfacial reaction is insertion of doped CeO₂ between YSZ and LSCF. Tsai et al. [1,2] and Brahim et al. [3] fabricated bilayered YSZ/doped CeO₂ electrolyte films using sputtering technique. Recently, Nguyen et al. obtained bilayered electrolyte films using slurry dip-coating technique [4,5] which is a wet ceramic process that is advantageous for fabrication of cost-effective SOFCs over physical processes. In the fabrication described by Nguyen et al., the slurry dip-coating technique was used for coating the doped CeO₂ films onto dense Sc₂O₃-stabilized ZrO₂ films prepared by pre-heating at 1300 °C. The authors have used EPD, which is known as a practical technique, to fabricate bilayered electrolyte films of YSZ with Sm₂O₃-doped CeO₂ (SDC) as a barrier layer. The EPD is a colloidal process with the accumulation of finely dispersed ceramic powders from suspension onto substrates in a DC electric field. Technical advantages of EPD include: simplicity of operation; short processing time; uniformity of the deposited films, even for large and complex forms; and control of the film thickness. Therefore, EPD seems to be a favorable method to fabricate electrolyte films for SOFCs operating at reduced temperatures with various stack designs such as a tubular cell stack. Until now, although the EPD has been used for single-layered electrolytes, no attempt has been made for bilayered electrolyte SOFCs. In the

* Corresponding author. Tel.: +81 86 251 8907; fax: +81 86 251 8907.
E-mail address: mm@cc.okayama-u.ac.jp (M. Matsuda).

present work, bilayered YSZ/SDC electrolyte films have been fabricated with EPD processes using YSZ and SDC applied layer by layer, then co-firing after deposition of two layers. This paper specifically describes electrophoretic fabrication of bilayered YSZ/SDC electrolyte films on non-conducting porous NiO–YSZ composite substrates, which can be used as an anode in reduced-temperature operating SOFC. The performance of the bilayered films is compared with that of single-layered YSZ electrolyte films after construction of anode-supported single cells using LSCF as a cathode.

2. Experimental

Porous NiO–YSZ composite substrates were fabricated by tape-casting a slurry consisting of mixed powders of NiO and YSZ (8 mol% Y_2O_3) with organic agents on polyethylene films followed by heating at 900 °C for 2 h. The fabricated substrates had porosity of ca. 56%. Prior to use, the porous substrates were coated with a graphite layer of less than 1 μm thickness because the electrical conductivity of the substrates was too low for an electrode in EPD processing.

Commercial powders, which were produced by Tosoh Corp. and Mitsuikinokoku Corp., were used for YSZ (8 mol% Y_2O_3) and SDC ($Ce_{0.8}Sm_{0.2}O_x$), respectively. The respective average sizes of those powders were ca. 0.3 and 1 μm ; 0.1 g of each powder was added to 50 mL of ethanol and dispersed using an ultrasonic vibration. The ethanol was used as-received with reagent grade.

In the present work, EPD was performed through a process based on electrophoretic filtration. Porous substrates with a graphite layer were put in YSZ-dispersed ethanol solutions. A stainless plate was used as a counter electrode, facing the surface without a graphite layer of the substrates. The distance between the graphite layer and stainless plate was 10 mm. The experimental setup was made according to previous reports [6,7]. Constant dc voltage of 600 V was applied between the electrodes, and the YSZ powders were deposited directly on the porous substrates. After EPDs of YSZ, the SDC powders were deposited on the as-deposited YSZ films on the porous substrates at dc voltage of 600 V in the same experimental manner as the YSZ. The obtained deposits were co-fired with the substrates at 1400 °C for 2 h. Thicknesses of the YSZ and SDC films were controlled according to the EPD time.

The deposits' microstructures and thickness before and after co-firing were examined using scanning electron microscopy

(SEM). The zeta-potentials of dispersed powders in the suspensions were measured using a Nano Zetasizer (Malvern Instruments, Ltd.).

To test the performance of the resultant bilayered YSZ/SDC films, a single cell was constructed using a LSCF cathode. The LSCF powders were prepared by a solid-state reaction of La_2O_3 , $SrCO_3$, Co_3O_4 and Fe_2O_3 at 1100 °C for 10 h. The La_2O_3 powder was pre-heated at 1000 °C for 5 h for dehydration of $La(OH)_3$ co-existing as an impurity. After they were ground sufficiently, the obtained LSCF powders were screen-painted on the SDC films, then heated at 850 °C for 4 h. The LSCF cathode layer thickness was around 30 μm . The single cell was mounted into an alumina tube with 9 mm inner diameter and 13 mm outer diameter and heated *in situ* at 800 °C for several hours in a reducing atmosphere to reduce NiO in the substrates into metallic Ni. Pyrex glass rings were used for sealing the cells. Measurements of cell performance were carried out at 700 °C with supplies of humidified (3% H_2O) hydrogen as fuel and air as oxidant. The gas-flow rate was constant at 50 $\text{cm}^3 \text{min}^{-1}$ during measurements. The electrode area was 28.3 mm^2 . Current–voltage curves were made using a galvanostat and a digital voltmeter. Current interrupt technique was used to estimate ohmic and overpotential losses in the cell performance separately. The current interrupt measurements were carried out in a two-electrode configuration, and conducted in parallel with the current–voltage curve measurements. When a constant-current load on the single cell was abruptly interrupted, the resulting voltage–time response was monitored. The ohmic and overpotential losses were estimated from the instantaneous rebound and time-dependent rebound in the voltage, respectively.

3. Results and discussion

Our preliminary experiments revealed that the YSZ and SDC powders dispersed in ethanol drifted to the cathodic electrode, indicating that those powders were positively charged in ethanol. The zeta potentials of YSZ and SDC in ethanol were measured, respectively, as ca. 40 and 23 mV. According to a previous report [8], a positive charge might result from adsorption of protons released in dissociation of H_2O contamination in ethanol, which was used as-received.

Before covering YSZ films with SDC, the sinterability of YSZ films formed electrophoretically on the porous NiO–YSZ composite substrates was investigated. Fig. 1 shows SEM

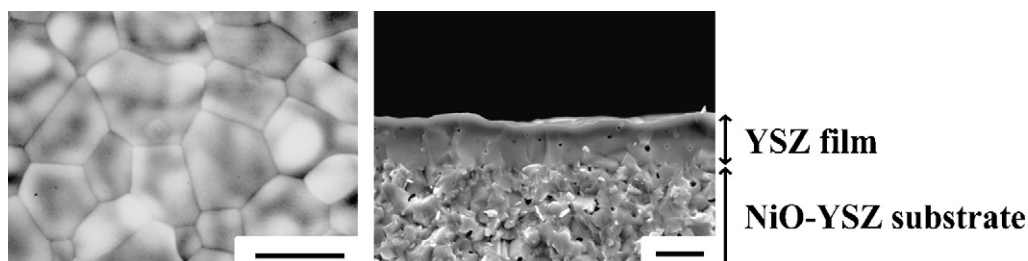


Fig. 1. SEM photographs of the surface and cross-section for YSZ films on the NiO–YSZ composite substrates after EPD followed by co-firing with the substrates (bars = 10 μm).

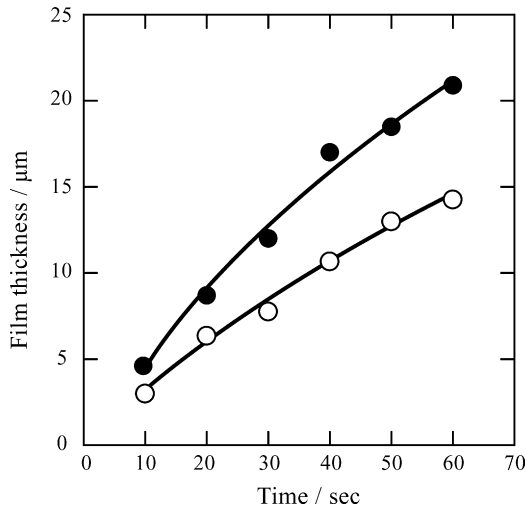


Fig. 2. EPD time dependence of film thickness for YSZ electrolyte films. Solid and open circles indicate film thickness before and after co-firing, respectively.

photographs of free and fracture surfaces of the YSZ films co-fired at 1400 °C with the substrates before EPD of SDC. The co-fired YSZ films had a dense body. No significant cracks or pin-holes were observed for the densified YSZ films. The YSZ films co-fired at 1400 °C were considered to be applicable to an electrolyte in SOFC.

Fig. 2 shows film thickness as a function of EPD time for the YSZ films before and after co-firing at 1400 °C. The film thickness increased concomitant with increased EPD time; it reached ca. 21 μm after 60 s EPD. The processing times were much shorter than those in other film fabrication processes. Therefore, the EPD is a time-saving film-fabrication process. Thicknesses of the as-deposited films were reduced after co-firing. The reducing ratios were about 35%.

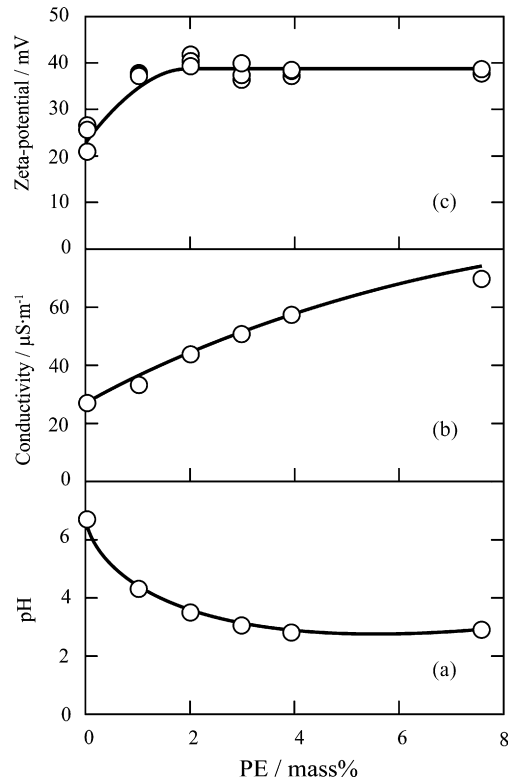


Fig. 3. pH (a), conductivities (b) and zeta-potentials (c) as a function of an amount of phosphate ester (PE) added for SDC-dispersed suspensions.

Although the SDC powders apparently drifted toward to the cathodic electrode in ethanol similar to the YSZ, no SDC powders were deposited on the as-deposited YSZ films on the porous substrates. A previous work [9] described EPD for depositing doped CeO₂ powders onto metallic Ni plates in ethanol with phosphate ester (PE) as a dispersant. Similar effects with PE have

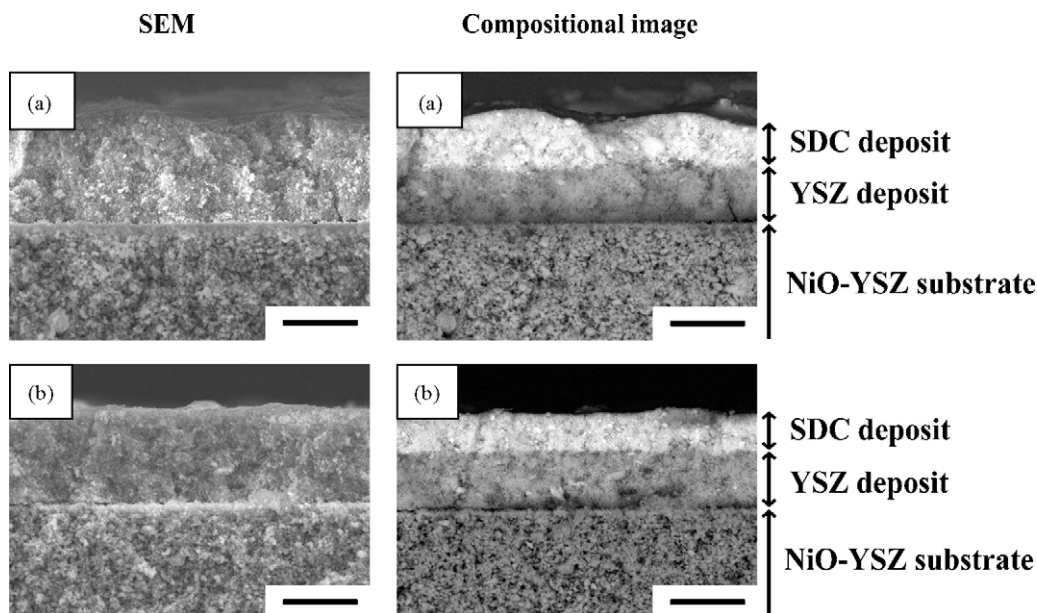


Fig. 4. Cross-sectional SEM photographs and compositional images for bilayered YSZ/SDC films before co-firing. For EPD of the SDC, phosphate ester (PE) was added to suspension: (a) 2 mass% and (b) 7.5 mass% (bars = 10 μm).

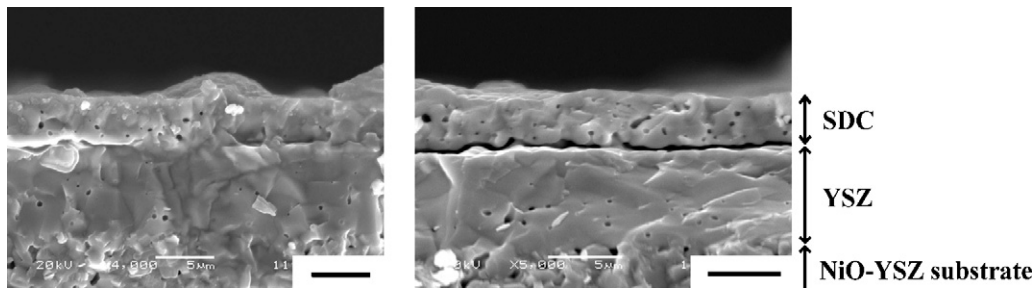


Fig. 5. Cross-sectional SEM photographs in different parts for the bilayered YSZ/SDC films after co-firing (Bars = 5 μm).

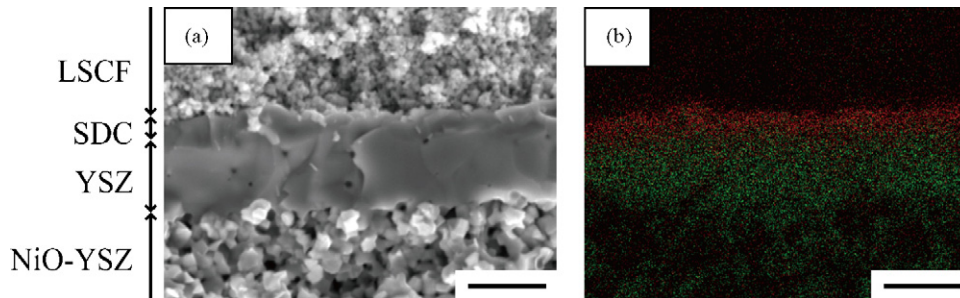


Fig. 6. Cross-sectional SEM photograph (a) and element distribution map (b) for the bilayered electrolyte films consisting of ca. 4 μm -thick YSZ and ca. 1 μm -thick SDC films after co-firing followed by testing cell performance. The red and green points in panel (b) denote Ce and Zr, respectively (Bars = 5 μm).

been observed for lead zirconia titanate perovskite compound [10]. According to previous reports by Zhitomirsky [11,12], the added PE donates protons to the surface of dispersed powders, charging the powders positively in organic solutions including ethanol. Zhitomirsky also points out that the PE acts as a steric dispersant by anchoring the long-chain molecules to the surface of the dispersed powders. Consequently, the addition of PE reportedly affects EPD. Therefore, in the present work, an amount of PE was added to the SDC-dispersed suspensions for the EPD.

Fig. 3 depicts the influences of the addition of PE on pH, conductivity and zeta-potential for the SDC-dispersed suspensions. Higher amounts of added PE were associated with lowered pH and increased conductivity. Those changes in pH and conductivity are reasonable because protons are released from the PE. The addition of PE also raised the zeta-potential of the dispersed SDC. As shown in Fig. 3(c), the zeta-potential increased to ca. 40 mV with 2 mass% PE, which was about twice that without the PE. According to a previous report [10], the addition of excess PE engenders a decrease in zeta-potential. However, as Fig. 3(c) shows, the zeta-potential of SDC in the present work was almost constant above 2 mass% PE, thereby indicating that the added amount of PE was within an appropriate range. In the present work, suspensions with 2 and 7.5 mass% PE were used for EPD of the SDC.

The SDC powders were deposited onto as-deposited YSZ films using PE-added suspensions. Fig. 4 shows cross-sectional SEM photographs and compositional images for bilayered YSZ/SDC films before co-firing. The SDC powders were packed densely within the film. A clear boundary was made between YSZ and SDC films. Observations using SEM also revealed that the surface of SDC films formed with 7.5 mass% PE was even,

whereas that with 2 mass% PE was uneven. In the experiments described below, suspensions with 7.5 mass% PE were used for the EPD of SDC.

In Fig. 5, two cross-sectional SEM photographs are shown for bilayered YSZ/SDC electrolyte films after co-firing. Each film was transformed in dense bodies after co-firing. However, as shown in Fig. 5, a delaminated part was visible in the bilayered films. The delamination resulted from differences in thermal expansion coefficient and sintering behavior between YSZ and SDC. Efforts were made in the present work to prevent delamination. As a result, it became apparent that the contact of SDC onto YSZ was improved by reducing the SDC films' thickness. Fig. 6 shows a cross-sectional SEM photograph and an element distribution map for bilayered films with ca. 1 μm -thick SDC film

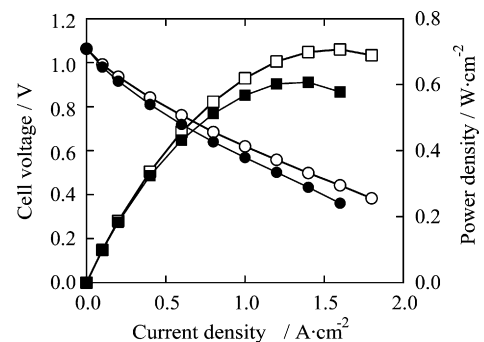


Fig. 7. Voltages (solid circle symbols) and output power densities (solid square symbols) at 700 $^{\circ}\text{C}$ as a function of current densities for anode-supported SOFC with bilayered electrolyte films consisting of ca. 4 μm -thick YSZ and ca. 1 μm -thick SDC films. For comparison, performance of anode-supported SOFC with ca. 4 μm -thick YSZ single-layered electrolyte is shown with open circle symbols for voltages and open square symbols for output power densities in the figure.

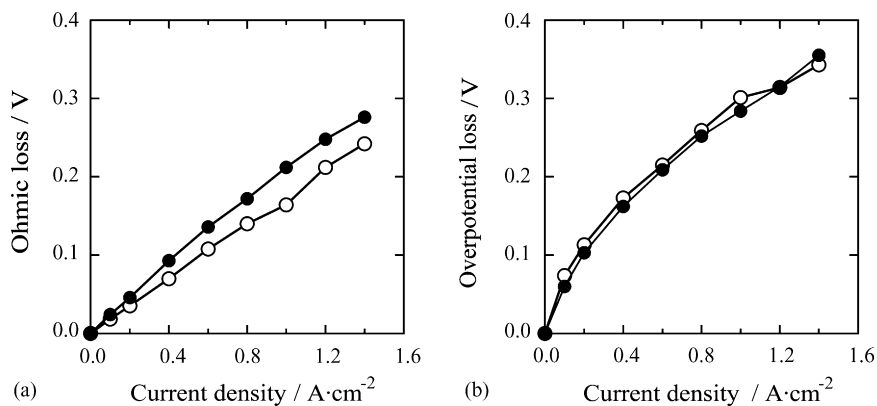


Fig. 8. Ohmic (a) and overpotential (b) losses in the cell performance at 700 °C shown in Fig. 7. The solid and open symbols indicate data for bilayered YSZ/SDC and for single-layered YSZ electrolyte SOFCs, respectively. The YSZ films were ca. 4 μm thick in the cells.

after co-firing followed by testing cell performance. Good contact and no delamination were observed at the interface. Previous studies observing reactants after prolonged treatments [13–15] have reported that doped CeO_2 reacts with YSZ at elevated temperatures. The reacting part may be, however, restricted within a narrow area around the interface for the bilayered films because of reduced co-firing time, even though the interfacial reaction occurred during co-firing in the present work. The interfacial reaction is discussed below using cell performance data.

Fig. 7 shows voltage and power density versus current density of a bilayered YSZ/SDC electrolyte SOFC operated at 700 °C. The respective thicknesses of YSZ and SDC films in the bilayered electrolyte were ca. 4 and 1 μm . For comparison, data of ca. 4 μm -thick single-layered YSZ electrolyte cells are shown in Fig. 7. No differences were apparent in the open-circuit voltages between the two types of cells, although differences were observed in the cell voltages and output power densities as a function of current density. The respective peak power densities of cells with and without the SDC as a barrier layer were 0.61 and 0.71 W cm^{-2} . As mentioned below, this resulted from a difference in losses attributable to ohmic resistance in the cell performance. However, the cell performance was sufficient for practical use of single cells. This result indicates that SOFCs with bilayered, electrophoretically fabricated YSZ/SDC electrolyte films have great potential for use at 700 °C. Durability of the bilayered YSZ/SDC electrolyte SOFC will be investigated in a future study.

Fig. 8(a) and (b) shows ohmic and overpotential losses in the cell performance of the two cells shown in Fig. 7, respectively. No difference was observed in the overpotential losses between the two cells. This is reasonable because the cathode and anode activation losses are responsible for overpotential losses. On the other hand, the ohmic losses for the cell with SDC were higher than those without SDC. The difference corresponded to an increase of ca. $3.33 \times 10^{-2} \Omega \text{cm}^2$ in area-specific resistance (ASR). The conductivity at 700 °C of the SDC film inserted as a barrier layer was calculated from the increased value of ASR. The estimated conductivity was ca. $3 \times 10^{-3} \text{ S cm}^{-1}$, which is one order of magnitude lower than the intrinsic value reported for SDC at 700 °C [16]. The estimation indicates that the undesirable increase in ASR is attributable to the interfacial reaction

between YSZ and SDC. Higher cell performance is, therefore, expected with less interfacial reaction. To achieve that goal, further investigations including EPD conditions are in progress to fabricate higher performance anode-supported SOFCs with bilayered YSZ/SDC electrolyte films.

4. Conclusions

In the present work, EPD processes based on electrophoretic filtration were applied to fabrication of bilayered YSZ/SDC electrolyte films on non-conducting porous NiO–YSZ composite substrates for reduced-temperature operating anode-supported SOFC. The bilayered electrolytes were fabricated using EPDs of YSZ in ethanol followed by SDC in PE-added ethanol onto the composite substrates. Delamination between YSZ and SDC films was avoidable by reducing thickness of the SDC films inserted as a barrier layer to ca. 1 μm . Maximum output power densities greater than 0.6 W cm^{-2} at 700 °C were attained on a bilayered electrolyte SOFC consisting of ca. 4 μm -thick YSZ and ca. 1 μm -thick SDC films.

Acknowledgements

This work was supported financially by a Grant-in-Aid for Scientific Research (B) (No. 16360331) from the Japan Society for the Promotion of Science (JSPS). This work was also supported in part by a Grant-in-Aid for Scientific Research (B) (No. 17350101) from JSPS and by the Okayama University 21st Century COE Program.

References

- [1] T. Tsai, E. Perry, S. Barnett, J. Electrochem. Soc. 144 (1997) L130–L132.
- [2] T. Tsai, S.A. Barnett, Solid State Ionics 98 (1997) 191–196.
- [3] C. Brahim, A. Ringuede, E. Gourba, M. Cassir, A. Billard, P. Briois, J. Power Sources 156 (2006) 45–49.
- [4] T.L. Nguyen, K. Kobayashi, T. Honda, Y. Iimura, K. Kato, A. Negishi, K. Nozaki, F. Tappero, K. Sasaki, H. Shirahama, K. Ota, M. Dokiya, T. Kato, Solid State Ionics 174 (2004) 163–174.
- [5] T.L. Nguyen, T. Kato, K. Nozaki, T. Honda, A. Negishi, K. Kato, Y. Iimura, J. Electrochem. Soc. 153 (2006) A1310–A1316.

- [6] M. Matsuda, T. Hosomi, K. Murata, T. Fukui, M. Miyake, *Electrochem. Solid-State Lett.* 8 (2005) A8–A11.
- [7] T. Hosomi, M. Matsuda, M. Miyake, *J. Eur. Ceram. Soc.* 27 (2007) 173–178.
- [8] H. Negishi, K. Yamaji, N. Sakai, T. Horita, H. Yanagishita, H. Yokokawa, *J. Mater. Sci.* 39 (2004) 833–838.
- [9] I. Zhitomirsky, A. Petric, Electrophoretic deposition of ceramic materials for fuel cell applications, *J. Eur. Ceram. Soc.* 20 (12) (2000) 2055–2061.
- [10] S. Dounghaw, T. Uchikoshi, Y. Noguchi, C. Eamchotchawalit, Y. Sakka, *Sci. Technol. Adv. Mater.* 6 (2005) 927–932.
- [11] I. Zhitomirsky, *Adv. Colloid Interf. Sci.* 97 (2002) 279–317.
- [12] I. Zhitomirsky, A. Petric, *J. Mater. Sci.* 39 (2004) 825–831.
- [13] Y. Hinatsu, T. Muromura, *Mater. Res. Bull.* 21 (1986) 1343–1349.
- [14] N.M. Sammes, G.A. Tompsett, Z. Cai, *Solid State Ionics* 121 (1999) 121–125.
- [15] N. Sakai, T. Hashimoto, T. Katsube, K. Yamaji, H. Negishi, T. Horita, H. Yokokawa, Y.P. Xiong, M. Nakagawa, Y. Takahashi, *Solid State Ionics* 143 (2001) 151–160.
- [16] V.V. Kharton, F.M.B. Marques, A. Atkinson, *Solid State Ionics* 174 (2004) 135–149.